# *Forme Fruste* Cor Triatriatum Dexter by Transesophageal Echocardiography and Its Impact on Percutaneous Heart Procedures: A Case Series

Benjamin M. Gold, MD, Dhaval R. Parekh, MD, Debra L. Kearney, MD, Guilherme V. Silva, MD, R. David Fish, MD, and Raymond F. Stainback, MD, *Houston, Texas*

## INTRODUCTION

Cor triatriatum dexter (CTD) is a rare congenital malformation of the right atrium (RA) in which the right venous valve is not resorbed, causing the RA to have two distinct chambers. It is often associated with other heart abnormalities, including atrial septal defects (ASDs). The Eustachian valve (EV) and Thebesian valve, guarding the inferior vena cava (IVC) and coronary sinus ostia, respectively, are normal remnants of the right venous valve in the postnatal heart. Incomplete resorption of the valve may leave excessively large but nonobstructive membranous remnants that connect to the atrial septum, herein defined as *forme fruste* CTD (ff-CTD). Occasionally, asymptomatic ff-CTD is incidentally detected in adults during transesophageal echocardiography (TEE) imaging procedures using standard planar imaging, as illustrated in cases 1-10 below. This anatomic variant has the potential to obstruct percutaneous heart procedures such as valve replacement and ASD closure.[1]

## METHODS

On the basis of observations from an index case (case 1), directed real-time three-dimensional (3D) TEE imaging of the right interatrial septum was performed to confirm ff-CTD whenever standard two-dimensional (2D) TEE images revealed an atrial septum Y sign (Figure 1). We differentiated ff-CTD from a prominent EV whenever a shelf-like membranous structure extended from the valve to the interatrial septum. The lab's database was searched for any prior TEE results from the same patient. All TEE exams in this single-hospital, inpatient laboratory study were performed by experienced, level III trained echocardiographers. However, only one investigator performed all of the TEEs with prospective real-time 3D TEE imaging of the ff-CTD cases reported herein.

## RESULTS

From a total of 1,470 TEE examinations performed by a single operator during the years 2013-18, we identified 10 patients (0.61%) with ff-CTD.

### Case Descriptions

An asterisk (*) indicates that a prior TEE, performed by a different level III echocardiographer, was retrospectively reviewed that did not indicate the presence of ff-CTD. In Figures 1-8 (paired with cases 1-8), the ff-CTD membrane (shown by the arrowhead) is attached to the atrial septum adjacent to the fossa ovalis, producing a telltale Y sign when the atrial septum is imaged just below the aortic root but above the coronary sinus (low four-chamber view). Illustrations for cases 9 and 10 are not included due to space limits, but Video images are available.

***Case 1*.** A 51-year-old woman with chest discomfort was found by transthoracic echocardiography (TTE) to have a small incidental secundum ASD. A TEE confirmed a 1.4-cm secundum ASD and an unusual ridge of tissue extending along the atrial septum to the ASD inferior margin (Figure 1A, Video 1). However, ff-CTD was not reported. An Amplatzer septal occluder device (St. Jude Medical, Saint Paul, MN) was successfully deployed under TEE guidance with 3D imaging to better define the atrial septum (Figure 1B, Video 2). Device deployment was difficult. The right disk of the septal occluder was nestled atop the ff-CTD ridge, in part because of redundant fossa ovalis tissue.

***Case 2*.** A 73-year-old female hemodialysis patient presented with weakness and syncope. TTE showed a patent foramen ovale (PFO) and right atrial (RA) thrombi involving the superior vena cava (SVC) and her RA dialysis catheter. Brain magnetic resonance imaging revealed multifocal cerebral infarcts, and TEE confirmed a PFO tunnel defect with right-to-left shunting, for which the patient was referred for percutaneous PFO closure. The initial TEE exam did not report ff-CTD. During TEE-guided placement of a 25-mm Amplatzer cribriform septal occluder (St. Jude Medical), the device had to be repositioned twice owing to difficulties aligning the left and RA discs. The device was ultimately deployed successfully. Procedural TEE (Figure 2A, Video 3) revealed an ff-CTD that had not been recognized during the initial TEE but that obviously complicated device deployment (Figure 2B, Videos 4-6).

## VIDEO HIGHLIGHTS

**Video 1:** The ff-CTD membrane is attached to the atrial septum adjacent to the fossa ovalis, producing a telltale Y sign with small adjacent ASD (case 1).

**Video 2:** The deployed ASD closure device adjacent to the ff-CTC (case 1).

**Video 3:** The ff-CTD membrane is attached to the atrial septum adjacent to the fossa ovalis, producing a telltale Y sign (case 2).

**Video 4:** Intracardiac echocardiography image shows improper canted device position (case 2).

**Video 5:** Intracardiac echocardiography image shows improper canted device position after further manipulation (case 2).

**Video 6:** A final transesophageal bicaval view confirms eventual stable device deployment (case 2).

**Video 7:** Two-dimensional TEE images in the midesophageal four-chamber view. **(A)** The ff-CTD membrane (*arrowhead*) is attached to the atrial septum adjacent to the fossa ovalis, producing a telltale Y sign (case 3).

**Video 8:** Large secundum ASD detected by 2D TEE (case 3).

**Video 9:** A 3D TEE image of ff-CTD adjacent to the large secundum ASE (case 3).

**Video 10:** TEE four-chamber view shows maldeployed Amplatzer device RA disk (case 3).

**Video 11:** TEE simultaneous orthogonal plane imaging shows malpositioned Amplatzer device within a large secundum ASD in a modified four-chamber view and bicaval views. Note the nearly 180° abnormal rotation of the closure device atrial disks, which span the ASD rather than sealing the ASD on both sides (case 3).

**Video 12:** TEE midesophageal four-chamber view shows the ff-CTD membrane attached to the atrial septum adjacent to the fossa ovalis, producing a telltale Y sign (case 4).

**Video 13:** TEE midesophageal four-chamber view shows the ff-CTD membrane attached to the atrial septum adjacent to the fossa ovalis, producing a telltale Y sign (case 4).

**Video 14:** Two-dimensional TEE image shows the ff-CTD membrane attached to the atrial septum adjacent to the fossa ovalis, producing a telltale Y sign (case 5).

**Video 15:** TEE 3D views of ff-CTD membrane (case 5).

**Video 16:** A slightly rotated TEE 3D partially en face atrial septum view shows the ff-CTD membrane dividing the fossa ovalis in this case (case 5).

**Video 17:** The ff-CTD membrane is attached to the atrial septum adjacent to the fossa ovalis, producing a telltale Y sign (case 7).

**Video 18:** Intracardiac echocardiography image shows improper canted device position (case 7).

**Video 19:** Intracardiac echocardiography image shows improper canted device position after further manipulation (case 7).

**Video 20:** A final TEE 3D view confirms stable Amplatzer device deployment.

**Video 21:** The ff-CTD membrane (*arrowhead*) attached to the atrial septum adjacent to the fossa ovalis, producing a telltale Y sign (case 8).

**Video 22:** TEE 3D view of ff-CTD membrane (case 8).

**Video 23:** The ff-CTD membrane attached to the atrial septum adjacent to the fossa ovalis, producing a telltale Y sign (case 9).

**Video 24:** TEE 3D view of ff-CTD membrane (case 9).

**Video 25:** The ff-CTD membrane attached to the atrial septum adjacent to the fossa ovalis, producing a telltale Y sign (case 10).

**Video 26:** Low transseptal catheter position adjacent to the ff-CTD, which affected catheter placement during TEE guidance (case 10).

**Video 27:** TEE 3D view of ff-CTD membrane (case 10).

**Video 28:** Two-dimensional TEE modified short-axis view of the aortic valve angulated toward the IVC and TV. The prominent EV terminates before the atrial septum.

**Video 29:** Three-dimensional TEE image showing prominent EV. The Eustachian ridge extends to the inferior margin of the interatrial septum; the EV does not.

**View the video content online at www.cvcasejournal.com.**

**Case 3.** A 27-year-old woman reported shortness of breath and atypical chest pain. A TTE revealed an isolated 2.2-cm secundum ASD with severe right-sided chamber enlargement and moderate pulmonary hypertension. The patient was referred for elective percutaneous ASD closure with an Amplatzer septal occluder device under TEE guidance. The device could not be deployed despite multiple attempts. Careful 2D and 3D TEE imaging (Figures 3A and 3B, Videos 7-9) ultimately revealed a prominent extension of the ff-CTD up to the inferior ASD margin. This previously unrecognized shelf-like structure prohibited seating of the device's right disk after successful left-disk deployment (Figures 3C and 3D, Videos 10 and 11). The procedure was aborted, and the patient was referred for surgical ASD closure, which was successful.

**Case 4*.** A 68-year-old man with a history of coronary artery bypass surgery and bioprosthetic aortic valve replacement presented with dizziness, weakness, and syncope. Initial imaging with TTE and TEE revealed severe bioprosthetic aortic valve stenosis and regurgitation, but ff-CTD was not reported. During subsequent successful TEE-guided valve-in-valve transcatheter aortic valve replacement, ff-CTD was incidentally detected by 2D and 3D TEE (Figures 4A and 4B, Videos 12 and 13).

**Case 5.** A 46-year-old woman with a remote history of mechanical mitral valve (MV) replacement for rheumatic MV disease presented with worsening right-sided heart failure from chronic severe rheumatic tricuspid valve (TV) regurgitation. Intraoperative TEE during minimally invasive TV replacement surgery revealed ff-CTD by 2D and 3D imaging (Figure 5, Videos 14-16). The TV replacement was successful, and ff-CTD did not interfere with the operation. The severely dilated RA and right ventricle (RV) enabled exceptionally detailed anatomic visualization of ff-CTD, which extended into the fossa ovalis region, seemingly without clinical consequences.

**Case 6*.** A 56-year-old woman with prior MV repair presented with symptomatic atrial fibrillation. A recent prior TEE for direct-current cardioversion guidance revealed severe annuloplasty ring mitral stenosis, but no comment was made about the possible presence of ff-

Video 1                                    Video 2
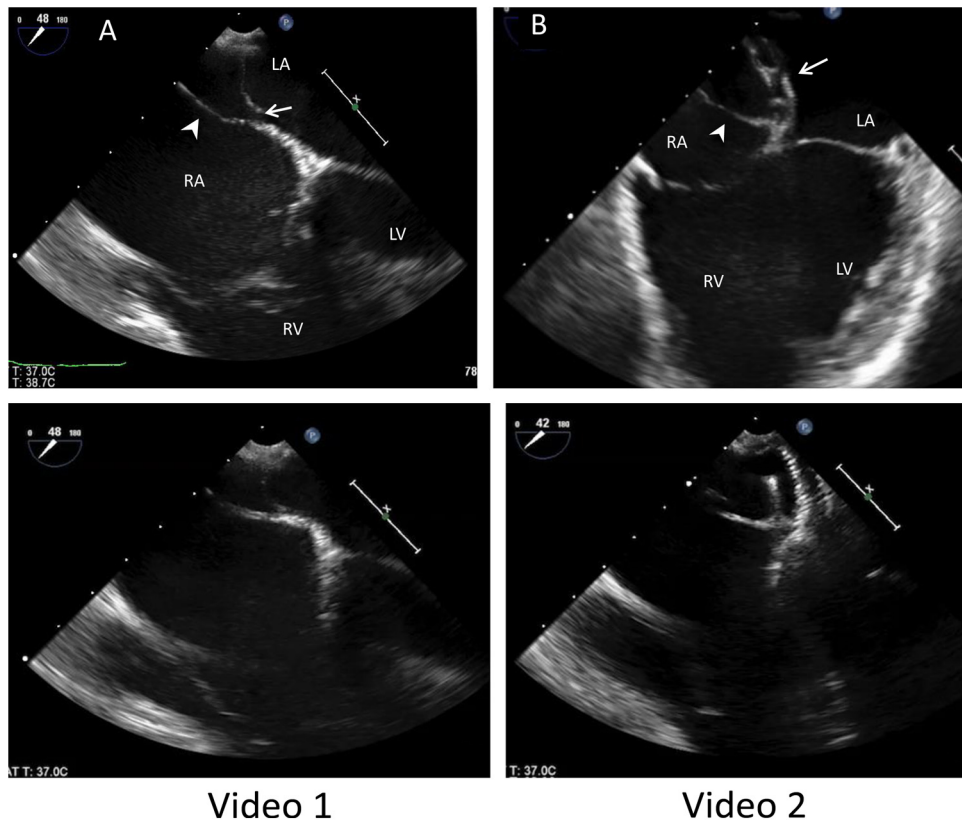
**Figure 1** Case 1. Two-dimensional TEE images in the midesophageal four-chamber view. The ff-CTD membrane (*arrowhead*) is attached to the atrial septum adjacent to the fossa ovalis, producing a telltale Y sign. **(A)** A small secundum ASD is also shown (*arrow*). **(B)** The deployed ASD closure device (*arrow*). *LA*, Left atrium; *LV*, left ventricle.

CTD. Subsequent intraoperative TEE during MV replacement surgery (Figure 6) showed a prominent EV with extension to the atrial septum, consistent with ff-CTD. The patient underwent successful MV replacement.

***Case 7\*.*** A 30-year-old woman with primary congenital hypomagnesemia, anoxic brain injury after infantile cardiac arrest, and deep vein thrombosis presented to the emergency room with a 2-week history of anorexia, nausea, vomiting, and dusky, blue-colored extremities. Her oxygen saturation was 83% on room air. A TTE with an agitated intravenous saline contrast study showed prominent right-to-left PFO shunting, confirmed by a TEE that revealed a prominent EV directing IVC flow across a PFO tunnel. However, ff-CTD was not reported. The patient underwent PFO closure with a 25-mm Amplatzer cribriform device. The procedural TEE exam showed ff-CTD (Figure 7A, Video 17). The RA disk deployment was initially difficult (Figure 7B, Videos 18-20) but ultimately successful after several positioning attempts.

***Case 8\*.*** A 54-year-old woman who had undergone total pentalogy of Fallot (tetralogy of Fallot with ASD) repair in childhood was found by TTE and magnetic resonance imaging to have a coronary sinus of Valsalva aneurysm obstructing the RV outflow tract. A preoperative TEE did not indicate ff-CTD. Subsequent intraoperative TEE (Figure 8, Videos 21 and 22) confirmed the other diagnoses and also incidentally revealed ff-CTD. The patient underwent surgical resection and repair of the right coronary sinus with a Hemashield woven patch (Atrium Medical, Hudson, NH). The ff-CTD was not resected, and the patient was discharged several days later in good condition.

***Case 9.*** A 73-year-old man with a history of prostate cancer, atrial fibrillation, coronary artery disease, and gastrointestinal bleeding was evaluated for percutaneous left atrial appendage (LAAP) closure-device placement. Preprocedural screening TEE revealed no LAAP thrombus, a small PFO, and prominent ff-CTD by 2D TEE (Video 23) and 3D TEE (Video 24) imaging. This anatomical variant was reported to the referring interventional cardiologist because it could interfere with a nearby transseptal puncture during the proposed LAAP device deployment. However, percutaneous LAAP closure was not pursued.

***Case 10\*.*** An 86-year-old woman with a history of atrial fibrillation, recurrent falls, and gastrointestinal bleeding was evaluated for LAAP closure-device placement. Preprocedural TEE showed acceptable LAAP morphology. However, 2D TEE (Videos 25 and 26) and 3D TEE (Video 27) performed during device insertion revealed ff-CTD, which repeatedly deflected the transseptal puncture needle to a position below the desired superior atrial septal location (Video 26). This necessitated multiple guide-catheter repositioning attempts and the placement and removal of three differently sized devices before correct insertion and LAAP occlusion could be accomplished, increasing fluoroscopy time.
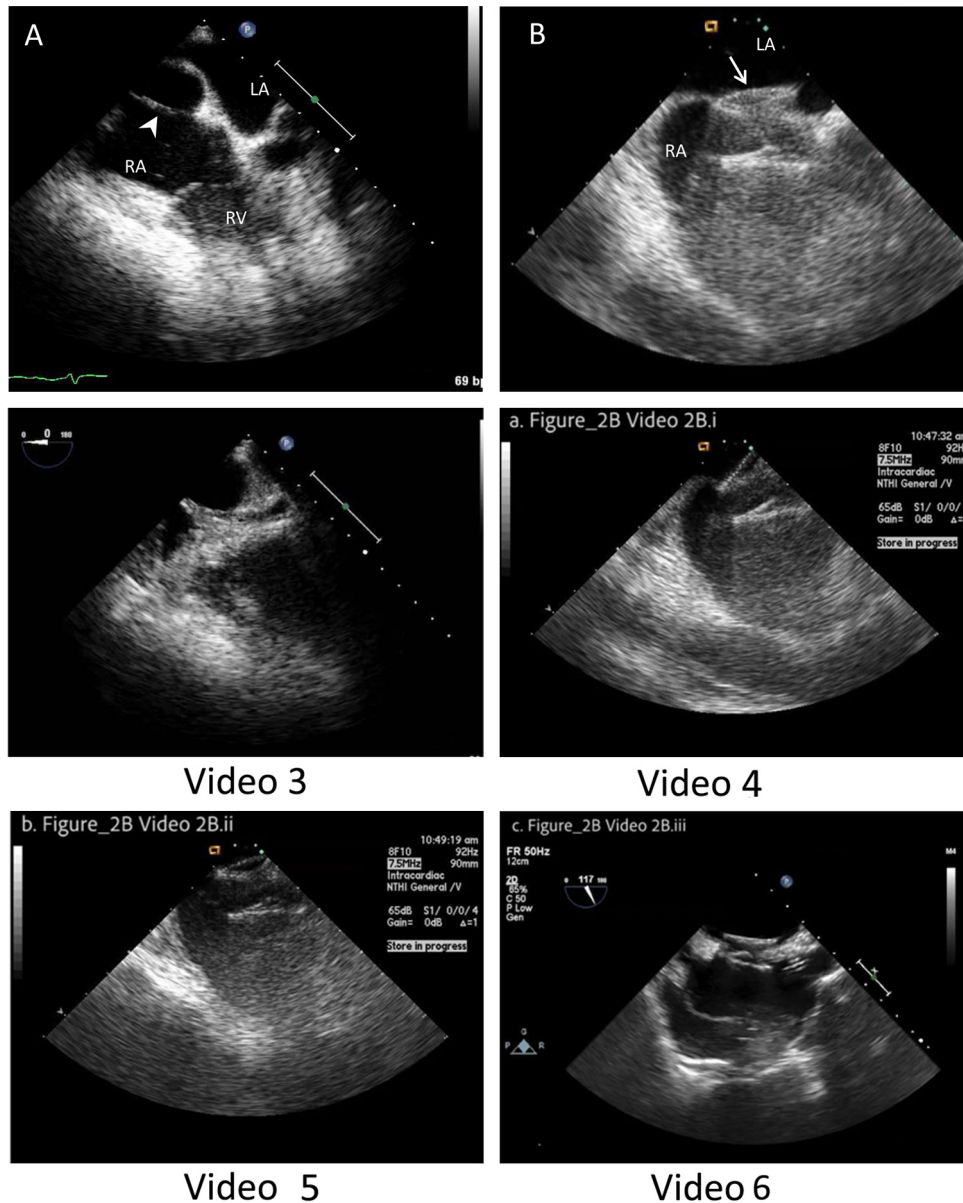
**Figure 2** Case 2. Two-dimensional TEE images in the midesophageal four-chamber view. **(A)** The ff-CTD membrane (*arrowhead*) is attached to the atrial septum adjacent to the fossa ovalis, producing a telltale Y sign. **(B)** PFO closure device with precarious and incomplete deployment (*arrow*). *LA*, Left atrium.

## DISCUSSION

### Epidemiology

Obstructive CTD is an extremely rare congenital heart abnormality in which the RA is divided into two chambers by the complete persistence of the right valve of the sinus venosus.[2] Whereas the prevalence of cor triatriatum sinister in patients with congenital heart disease is between 0.1% and 0.4%,[3,4] the true prevalence of CTD remains unknown, although estimates place it at < 0.01%.[1] Only 14 cases were reported between 1897 (when it was first characterized by Chiari) and 1972, all but one of which were identified postmortem.[2]

With the advent of echocardiography, CTD diagnoses have become more common. Often, CTD is associated with other right-sided heart malformations, including Ebstein anomaly, and stenosis or atresia of the tricuspid or pulmonary valves with a hypoplas-

tic RV.[2,4] Only a few cases of truly obstructive CTD in adult patients have been reported.[5] However, incidentally detected isolated nonobstructive ff-CTD has been reported more frequently as a clinically insignificant anatomic variant that can be confused with a cardiac mass.[6]

### Embryology and Anatomy

The RA develops early in fetal life when the right horn of the sinus venosus fuses with the primitive atrium. The sinus venosus is a quadrangular cavity that precedes the RA. The left horn of the sinus venosus becomes the coronary sinus and oblique vein of the left atrium. The right horn transports venous blood from the right anterior cardinal vein (which becomes the SVC), right vitelline vein (which becomes the IVC), and right umbilical vein (which eventually
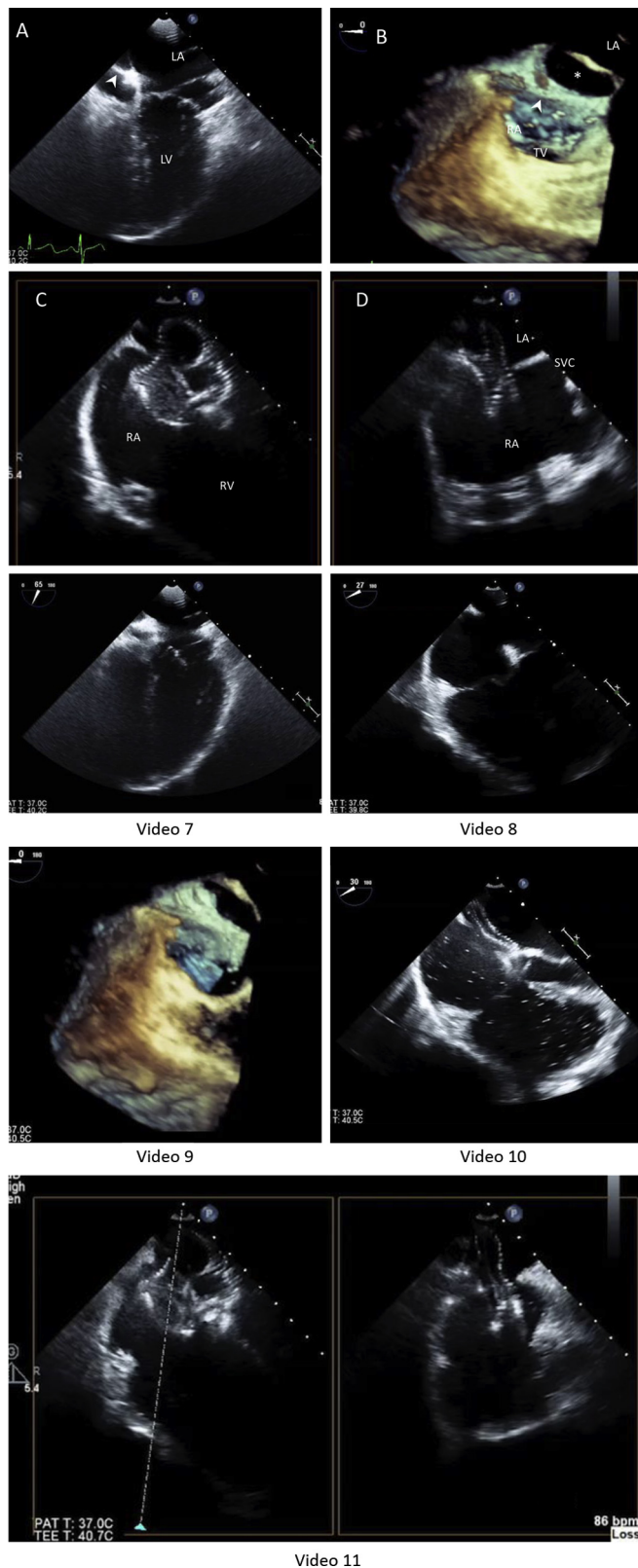
**Figure 3** Case 3. Two-dimensional TEE images in the midesophageal four-chamber view. **(A)** The ff-CTD membrane (*arrowheads*) is attached to the atrial septum adjacent to the fossa ovalis, producing a telltale Y sign. **(B)** Large secundum ASD detected by 3D TEE (*). Simultaneous orthogonal plane imaging shows malpositioned Amplatzer device within a large secundum ASD in modified **(C)** four-chamber view and **(D)** bicaval view. Note the nearly 180° abnormal rotation of the closure device atrial disks, which span the ASD rather than sealing the ASD on both sides. *LA*, Left atrium; *LV*, left ventricle.

**Video 12**        **Video 13**
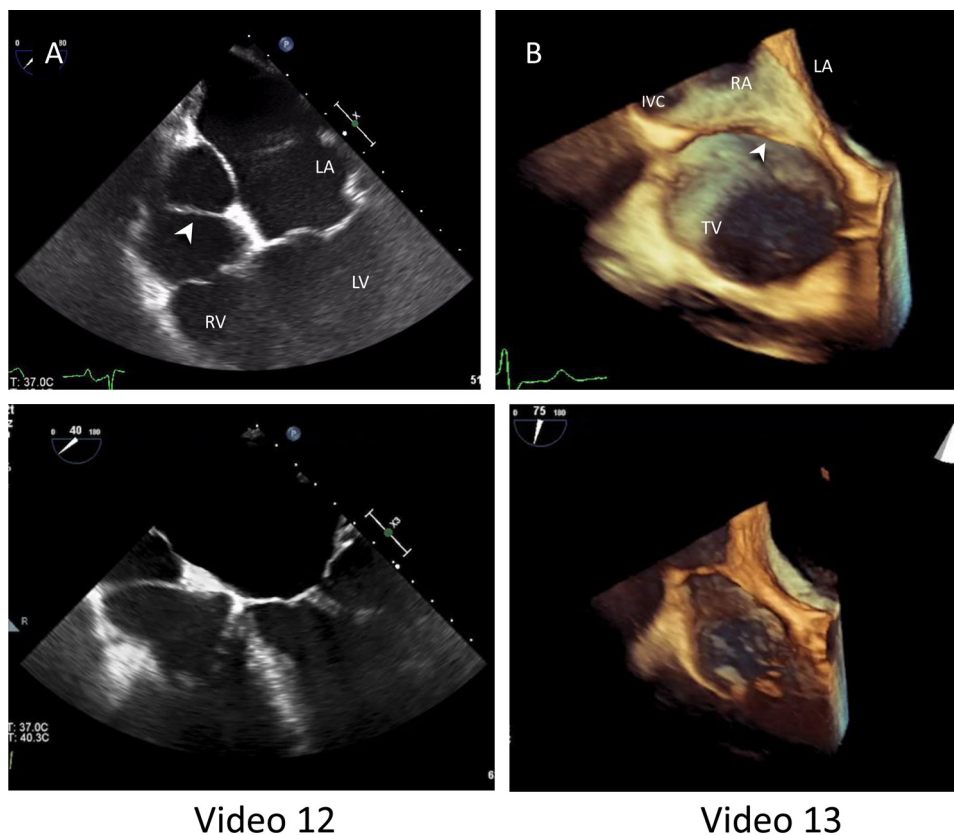
**Figure 4** Case 4. Two-dimensional TEE image **(A)** in the midesophageal four-chamber view shows the ff-CTD membrane (*arrowhead*) attached to the atrial septum adjacent to the fossa ovalis, producing a telltale Y sign. **(B)** TEE 3D views of ff-CTD membrane (*arrowhead*) using a semi–en face view of the atrial septum and TV annulus modified to best show the defect. *LA*, Left atrium; *LV*, left ventricle.

obliterates) to the primitive RA. The sinoatrial orifice, surrounded by the left and right venous valves, is the communication between the right horn of the sinus venosus and the primitive RA. The left venous valve eventually merges with the septum secundum, separating the left and right atria. The right venous valve partitions the RA into two chambers, allowing oxygenated blood from the umbilical vein to pass from the IVC across the PFO into the left atrium and to the systemic circulation. The right horn of the sinus venosus joins with the expanding RA, becoming a smooth-walled venous sinus, and the primitive RA becomes the RA appendage. During normal development, the right venous valve regresses between weeks 9 and 15, leaving the crista terminalis in front of the SVC superiorly and the EV of the IVC and the Thebesian valve of the coronary sinus inferiorly.[2,4,7]

In extensive, potentially obstructive CTD, the entire right venous valve persists at the sinoatrial orifice, running from the SVC to the IVC, resulting in division of the RA into an inlet portion receiving venous flow from the venae cavae and an outlet portion communicating with the RA appendage and TV.[8] Incomplete or partial persistence of the right venous valve can result in a prominent EV whose margins variably extend superiorly along the crista terminalis and anteriorly merge with the Thebesian valve. Often a prominent EV can mimic CTD on TTE and TEE if the RA appears septated.[9] However, in CTD, the partitioning membrane is attached to the interatrial septum, whereas a prominent EV (Figures 4 and 5) has no such attachment.[10,11] The CTD dividing membrane can range from small to large, may contain fenestrations or be intact, and may obstruct

blood flow to the RV. It can be shaped like a diaphragm, funnel, or band. If the membrane is extensively fenestrated and weblike in appearance, it is called a Chiari network.[7] Herein, we define ff-CTD as incomplete persistence of the right venous valve to the extent that it attaches to the atrial septum, typically along the anterior-inferior margin, with no associated obstruction (Figure 2).

### Clinical Manifestations

The degree to which CTD causes symptoms depends on the amount of obstruction in the RA. In patients with severe obstruction, hypoxia is often detected in infancy, and corrective surgery must be performed immediately.[4,12] In patients with an ASD, a large EV or ff-CTD can increase right-to-left shunting, causing cyanosis in infancy and requiring treatment.[11] However, if the CTD membrane is fenestrated or less extensive, as in ff-CTD, the lesion is often recognized only incidentally on echocardiographic imaging or during surgery or autopsy.[4] In these cases, the malformation is asymptomatic and hemodynamically insignificant and does not require treatment in isolation.

The rise in percutaneous ASD repairs may be giving ff-CTD new clinical relevance. The association between CTD and ASD is strong and well documented in the literature.[1,2] Nonobstructive CTD, herein referred to as ff-CTD, has recently been shown to interfere with the deployment of atrial septal occluder devices, both in a series of case reports[1,9,10,13] and in several of our own cases. In the current series, two cases of ff-CTD (cases 2 and 4) were detected incidentally by TEE during a percutaneous procedure for structural heart disease.
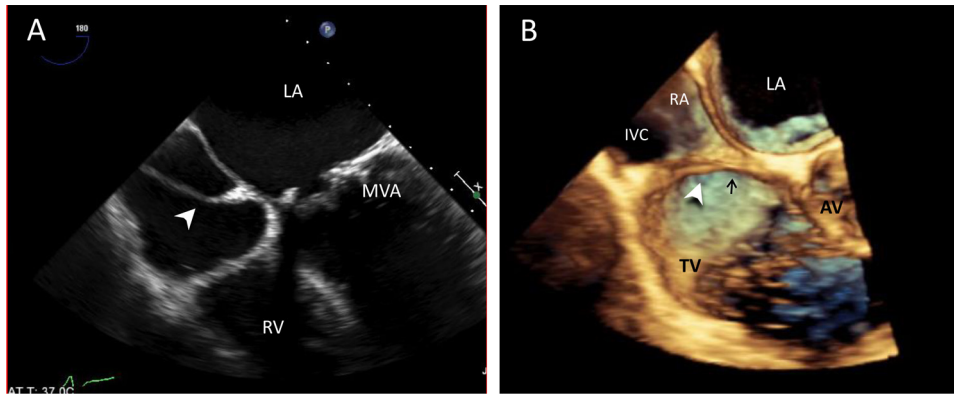
Video 14

Video 15

Video 16
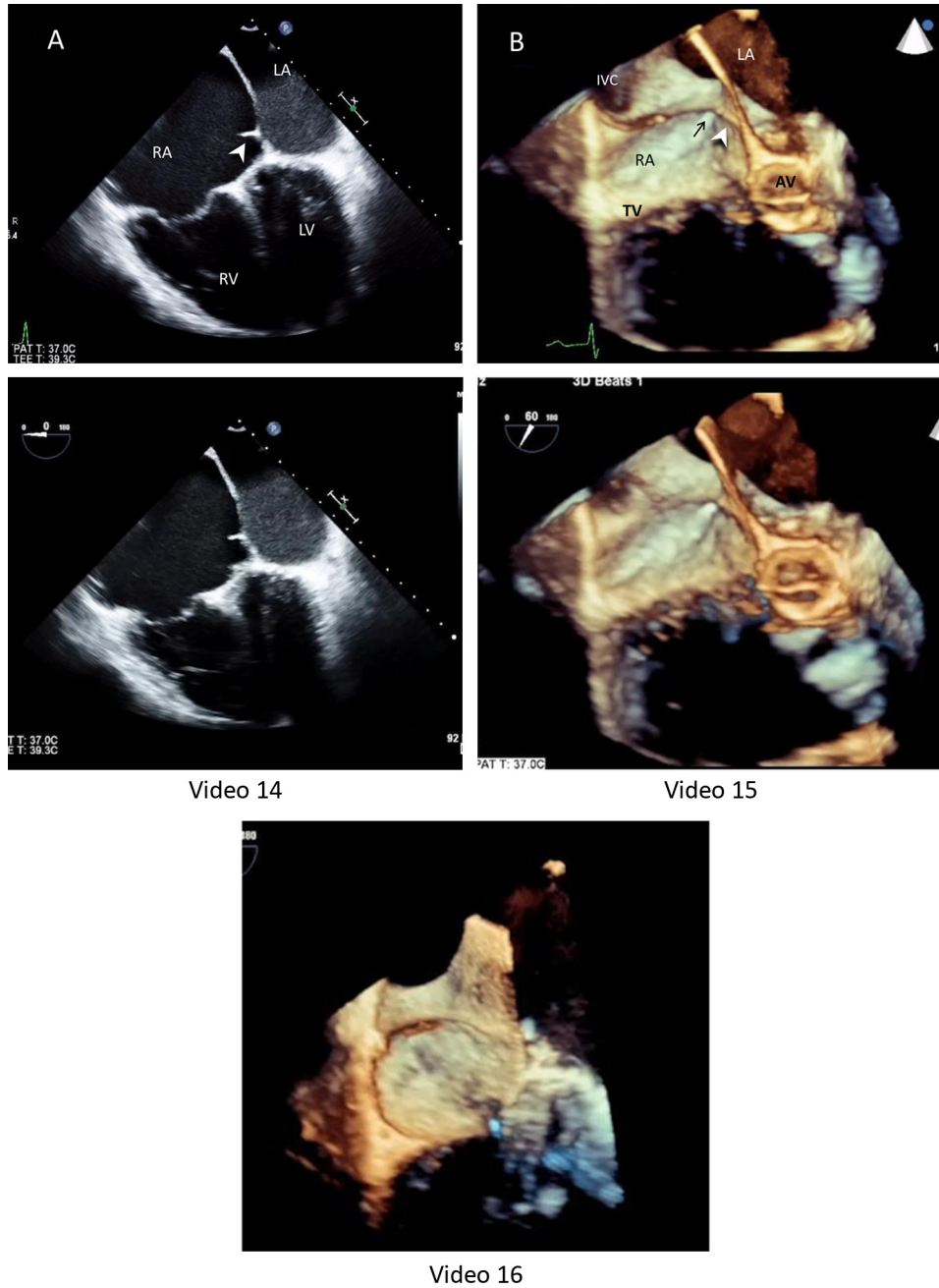
**Figure 5** Case 5. Two-dimensional TEE images **(A)** show the ff-CTD membrane (*arrowhead*) attached to the atrial septum adjacent to the fossa ovalis, producing a telltale Y sign when the atrial septum is imaged just below the aortic root but above the coronary sinus (low four-chamber view). **(B)** TEE 3D views of ff-CTD membrane (*arrowhead*) using a semi–en face view of the atrial septum and TV annulus to best show the defect; *black arrow* = coronary sinus. *AV*, Aortic valve *LA*, left atrium; *LV*, left ventricle.

Thus, the discovery of ff-CTD in a patient with ASD may affect the decision whether to attempt percutaneous repair or to proceed directly to surgical repair.

The current evidence is mixed regarding percutaneous ASD repair in patients with concomitant ff-CTD. Some investigators recommend waiting to close ASDs percutaneously until ff-CTD has been corrected surgically or by percutaneous balloon ablation[14]; however, successful percutaneous ASD closures have been reported in patients with uncorrected ff-CTD.[15] Other reports describe success with steer-

able radiofrequency ablation catheterization in the RA (via the femoral vein) to displace the EV against the RA wall, allowing free passage of the septal occluder.[16] However, even if the ff-CTD membrane is disrupted, the patient may still have inadequate rims around the caval orifice for percutaneous ASD closure, necessitating open surgery.[1]

Our findings are consistent with those of recently published studies suggesting that CTD (ff-CTD as defined herein) patients who undergo percutaneous heart procedures have a range of clinical outcomes. Six

**Figure 6** Case 6. Two-dimensional TEE image **(A)** shows the ff-CTD membrane (*arrowhead*) attached to the atrial septum adjacent to the fossa ovalis, producing a telltale Y sign when the atrial septum is imaged just below the aortic root but above the coronary sinus (low four-chamber view). **(B)** 3D TEE views of ff-CTD membrane (*arrowhead*) using a semi–en face view of the atrial septum and TV annulus to best show the defect; *black arrow* = coronary sinus. *AV*, Aortic valve *LA*, left atrium; *MVA*, MV annuloplasty ring.



Video 17

Video 18

Video 19

Video 20
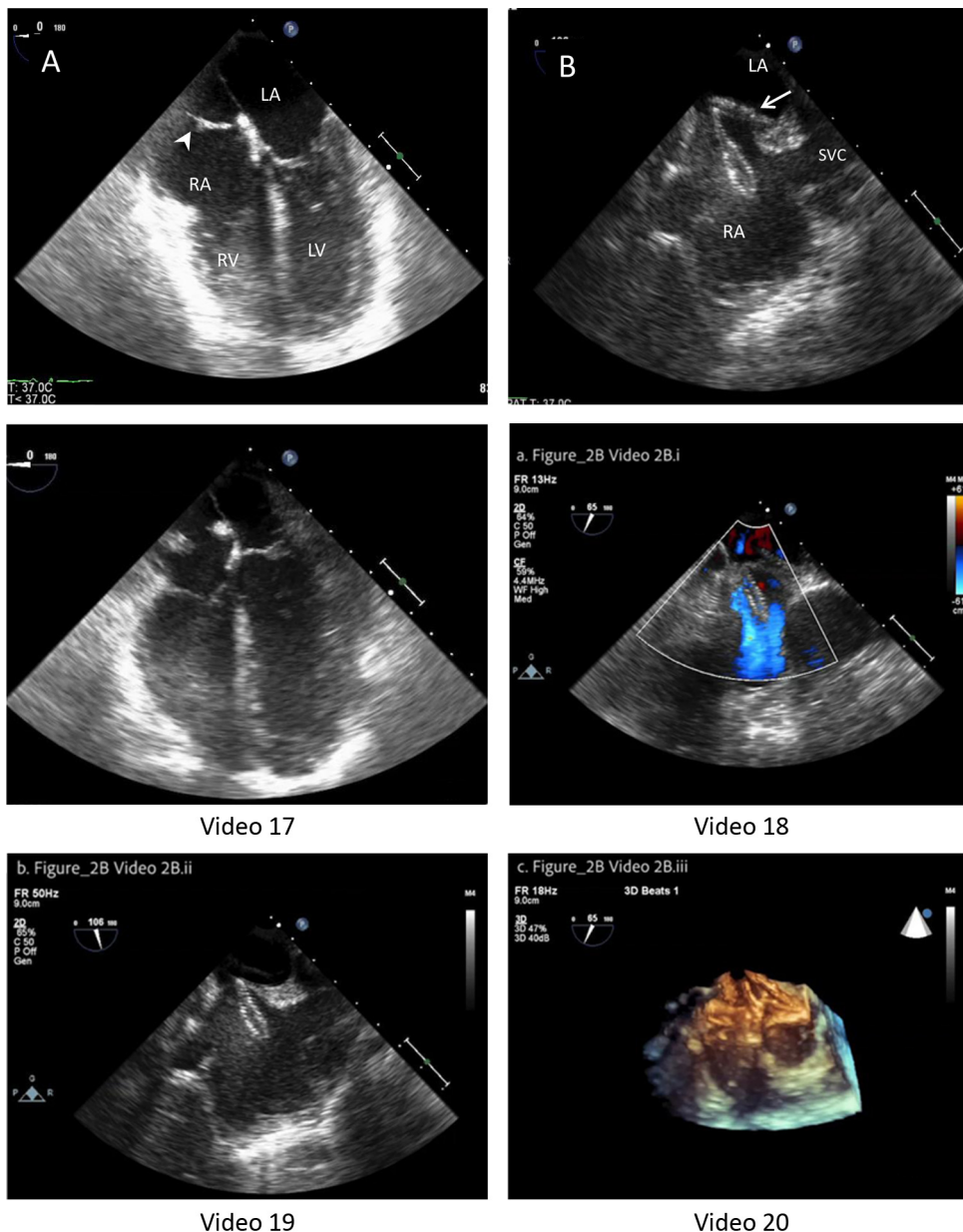
**Figure 7** Case 7. Two-dimensional TEE images in the midesophageal four-chamber view. **(A)** The ff-CTD membrane (*arrowhead*) is attached to the atrial septum adjacent to the fossa ovalis, producing a telltale Y sign. **(B)** TEE in a bicaval view shows PFO closure device with precarious and incomplete deployment (*arrow*). *LA*, left atrium; *LV*, left ventricle.

Video 21                              Video 22
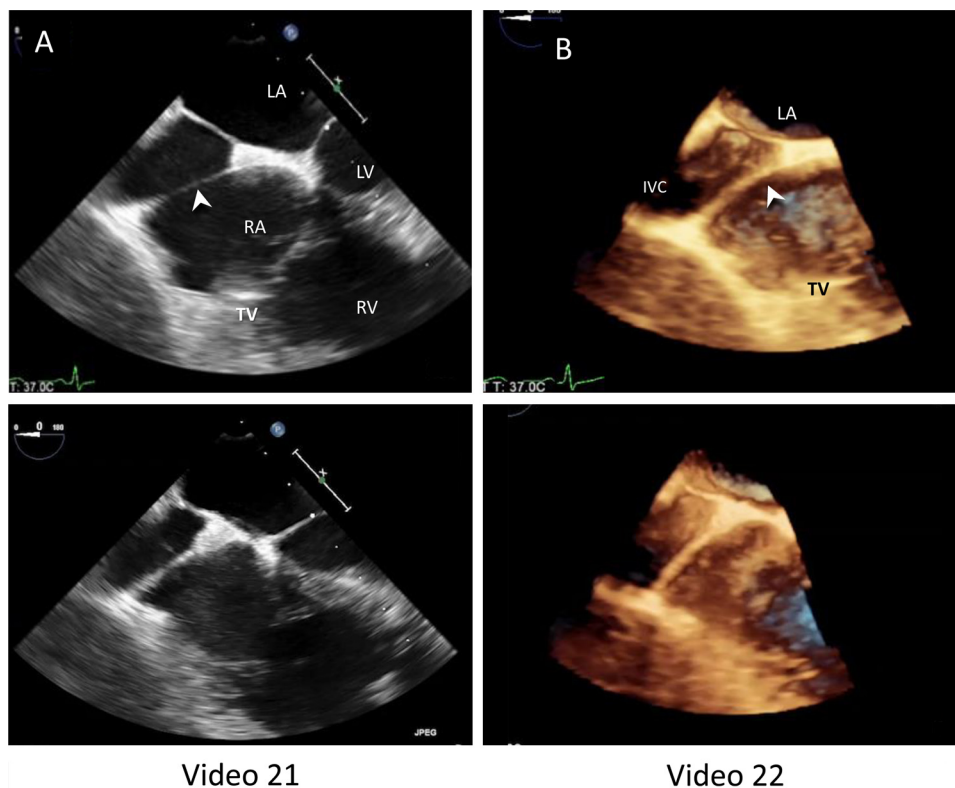
**Figure 8** Case 8. TEE images. **(A)** The ff-CTD membrane (*arrowhead*) attached to the atrial septum adjacent to the fossa ovalis, producing a telltale Y sign by 2D TEE. **(B)** TEE 3D view of *the* ff-CTD membrane (*arrowhead*) using a semi–en face view of the atrial septum and TV annulus to best show the defect. *LA*, Left atrium; *LV*, left ventricle.



Video 28                              Video 29
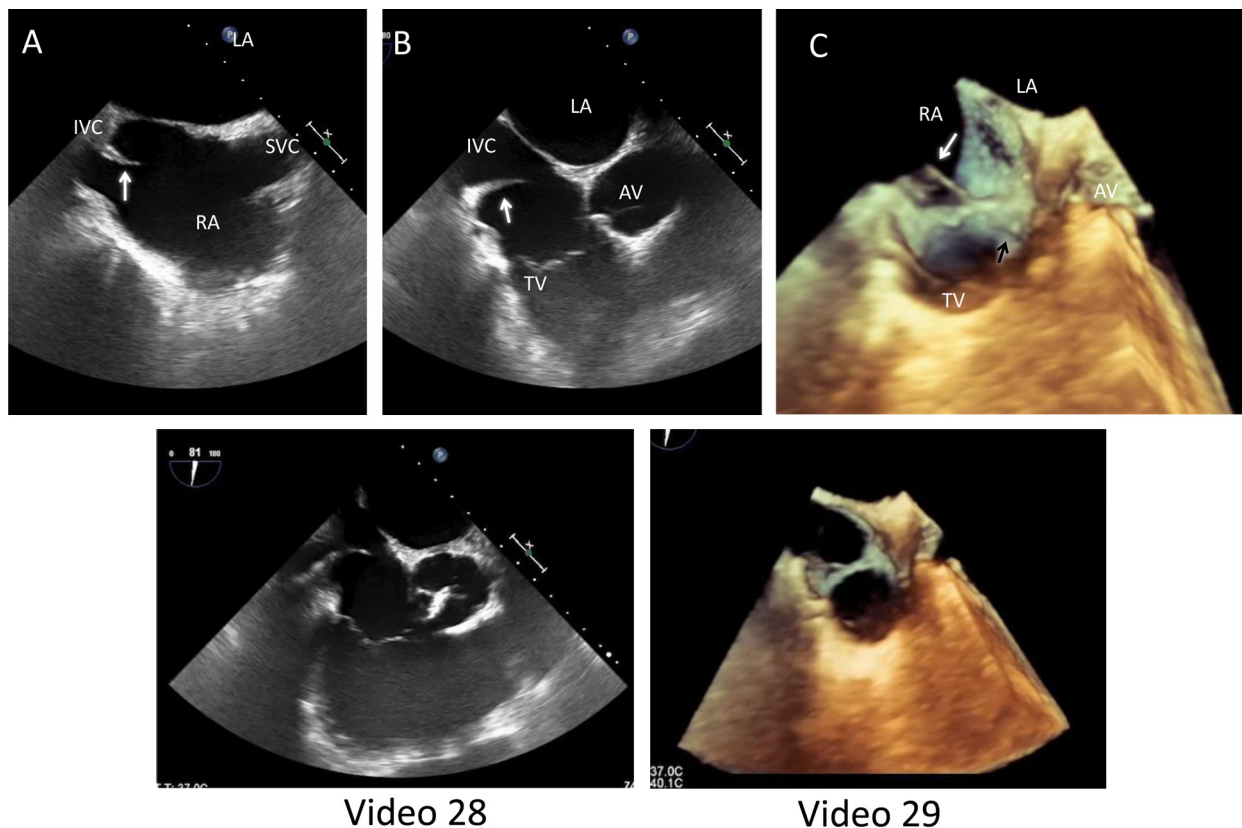
**Figure 9** Case 9. Prominent EV (*white arrows*). **(A)** 2D TEE in midesophageal bicaval view, showing the IVC, SVC, RA, left atrium (LA), TV, and aortic valve (AV). **(B)** 2D TEE modified short-axis view of AV angulated toward the IVC and TV to show prominent EV (*arrow*), which terminates before the atrial septum. **(C)** 3D TEE image showing prominent EV, Eustachian ridge (*black arrow*), and coronary sinus. The Eustachian ridge extends to the inferior margin of the interatrial septum; the EV does not.
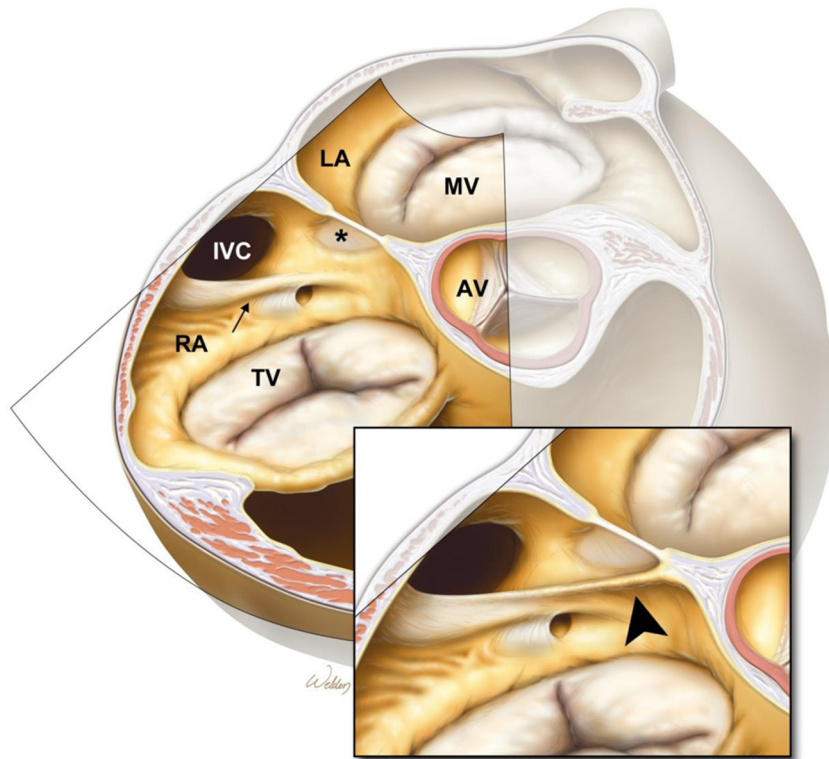
**Figure 10** Illustration of modified 3D TEE reconstruction cut plane that is not a "standard" direct en face view of the interatrial septum but a modified view to better illustrate the relationship between the atrial septum and fossa ovalis (*) of either a prominent EV (*small arrow*) or the ff-CTD membrane illustrated in the inserted drawing (*arrowhead*), which extends onto the atrial septum and creates the Y sign on planar images. *AV*, Aortic valve; *LA*, left atrium. ©Copyright, Baylor College of Medicine, printed with permission. Illustration by Scott A. Weldon, MA, CMI, FAMI.

of our 10 patients had either an ASD or a PFO, and four of the 10 were referred for Amplatzer septal occluder device placement. In three of these four patients, ff-CTD significantly affected the positioning of the device, leading to either abortion of the procedure (in one) or multiple repositioning attempts (in all). In addition, two of our 10 patients were referred for LAAP closure-device placement, and one underwent it. This patient had a difficult device placement due to ff-CTD, which involved multiple repositioning attempts and the use of several different LAAP closure devices. Although device placement was ultimately successful in four out of five procedures, each case involved a prolonged procedure time and radiation exposure.

In all 10 of our cases, there appeared to be anterior extension of the EV along the Eustachian ridge (containing the tendon of Todaro), to the atrial septum at the anterior inferior fossa ovalis limbus. The proximity of these structures is an important anatomic concept. Small anatomic variations in this small region of the heart, including ff-CTD, are usually of no clinical significance unless a percutaneous atrial septal procedure is being considered. Differentiating between ff-CTD and a prominent EV or Eustachian ridge may be difficult. Figures 9A and 9B show a typical prominent EV, which was incidentally detected in a 47-year-old man undergoing TEE for possible endocarditis. Both 2D TEE (Figures 9A and 9B, Video 28) and 3D TEE (Figure 9C, Video 29) imaging shows termination of the prominent EV atop the Eustachian ridge, without extension to the atrial septum. Because of its proximity to the inferior fossa ovalis, a prominent

Eustachian ridge could potentially interfere with atrial septal closure-device placement; case 3 may be an example of such interference. A prominent Eustachian ridge alone is a potential cause of difficult closure-device deployment, and it may have contributed to failed device deployment in our case.[17] The potential clinical implications of a prominent EV without ff-CTD is illustrated in Figure 9; this common morphological variant should be further examined in prospective studies.

### Three-Dimensional TEE Imaging Considerations

Echocardiography, regardless of modality (transthoracic, transesophageal, or intracardiac), is considered essential for patient selection and for monitoring transcatheter procedures.[18-20] TEE with real-time 3D imaging is particularly well suited for appreciating complex 3D anatomic variants and surrounding structures,[21,22] which may be difficult to discern by planar imaging alone. In our patients with suspected ff-CTD, 3D TEE was performed because of the unusual septated appearance of the basal atrial septum (Y sign) near the aortic root (Figure 1). Therefore, additional 3D TEE imaging may not always be warranted in patients with typical anatomy in this region.

When it comes to standardized 3D TEE imaging of the RA septum, there appears to be a consensus[19-24] that atrial septal communications viewed from the RA should be displayed by the Netter approach (https://netterimages.com/right-atrium-and-right-ventricle-unlabeled-cardiology-hypertension-frank-h-netter-738.html). This is an en face view toward the atrial septum, with the SVC near the top of the image,

the IVC near the bottom, and the TV annulus on the right. Although standard views can be helpful, multiple 3D views are recommended to better elucidate unusual anatomy.[24] In our patients, we found that a semi–en face view of the combined EV, atrial septum, and TV annulus complex (showing the Eustachian ridge and coronary sinus os, when possible) best described the ff-CTD membrane; this is illustrated in Figure 10.

## CONCLUSION

Our study shows the unique 2D and 3D TEE features of ff-CTD, including examples of near failure and failure to deploy percutaneous ASD closure devices under TEE guidance. Six of 10 patients had an atrial septal communication (ASD or PFO). We performed atrial septal 3D TEE imaging whenever a conventional 2D TEE atrial septal Y sign raised suspicion of ff-CTD. Therefore, even in this small case series, we confirmed a previously recognized association between atrial septal communications and ff-CTD. Experienced level III TEE operators whose exams were available for review within the same lab did not recognize ff-CTD on a prior TEE study in seven of our 10 cases. Therefore, clinically silent ff-CTD may be more prevalent than has been previously reported. Even clinically silent ff-CTD can interfere with percutaneous atrial septal closure-device deployment, as described in three of the four cases in which percutaneous atrial septal closure was performed or attempted. When 2D TEE imaging arouses suspicion (Figure 1), additional anatomically directed semi–en face 3D TEE views (Figure 2) can confirm and further define ff-CTD. Because evidence suggests that ff-CTD is strongly associated with atrial septal abnormalities,[2] prospective use of a combined 2D and newer 3D TEE imaging approach may improve ff-CTD detection, as well as the accuracy of TEE procedural guidance during atrial septal closure-device deployment and possibly other invasive procedures involving a percutaneous transatrial septal approach. Further, larger studies may be useful to address these questions.

## ACKNOWLEDGMENT

## SUPPLEMENTARY DATA

Supplementary data to this article can be found online at https://doi.org/10.1016/j.case.2019.05.004.

## REFERENCES

1. Vukovic PM, Kosevic D, Milicic M, Jovovic L, Stojanovic I, Micovic S. Cor triatriatum dexter and atrial septal defect in a 43-year-old woman. Tex Heart Inst J 2014;41:418-20.
2. Hansing CE, Young WP, Rowe GG. Cor triatriatum dexter. Persistent right sinus venosus valve. Am J Cardiol 1972;30:559-64.
3. Krasemann Z, Scheld HH, Tjan TD, Krasemann T. Cor triatriatum: short review of the literature upon ten new cases. Herz 2007;32:506-10.
4. Hoye DJ, Wilson EC, Fyfe DA, Guzzetta NA. Cor triatriatum dexter: a rare cause of neonatal cyanosis. Anesth Analg 2010;110:716-8. discussion 718.
5. Sarikouch S, Blanz U, Sandica E, Beerbaum P. Adult congenital disease: cor triatriatum dextrum. J Thorac Cardiovasc Surg 2006;132:164-5.
6. Yarrabolu TR, Simpson L, Virani SS, Arora H, Navarijo J, Stainback RF. Cor triatriatum dexter. Tex Heart Inst J 2007;34:383-5.
7. Shirani J, Acharya YR, Kalyanasundaram A, Pourmoghadam KK. Cor triatriatum 2006. Available at: http://emedicine.medscape.com/article/154168-overview. Accessed May 11, 2017.
8. Burton DA, Chin A, Weinberg PM, Pigott JD. Identification of cor triatriatum dexter by two-dimensional echocardiography. Am J Cardiol 1987;60:409-10.
9. Martinez-Quintana E, Rodriguez-Gonzalez F. Focusing on cor triatriatum dexter and atrial septal defects. Tex Heart Inst J 2014;41:567-8.
10. Martinez-Quintana E, Rodriguez-Gonzalez F, Marrero-Santiago H, Santana-Montesdeoca J, Lopez-Gude MJ. Cor triatriatum dexter versus prominent Eustachian valve in an adult congenital heart disease patient. Congenit Heart Dis 2013;8:589-91.
11. Yavuz T, Nazli C, Kinay O, Kutsal A. Giant eustachian valve with echocardiographic appearance of divided right atrium. Tex Heart Inst J 2002;29:336-8.
12. Carton AJ, Gonzalez Rocafort A, Rubio D, Garcia-Guereta L. Persistent embryonic right venous valve giving a cor triatriatum dexter appearance in a cyanotic neonate. J Thorac Cardiovasc Surg 2011;142:e147-8.
13. Ebeid MR. Percutaneous catheter closure of secundum atrial septal defects: a review. J Invasive Cardiol 2002;14:25-31.
14. Savas V, Samyn J, Schreiber TL, Hauser A, O'Neill WW. Cor triatriatum dexter: recognition and percutaneous transluminal correction. Cathet Cardiovasc Diagn 1991;23:183-6.
15. Ebeid MR, Braden DS, Gaymes CH, Heath B, Joransen JA. Postsurgical use of Amplatzer septal occluder in cyanotic patients with pulmonary atresia/intact ventricular septum: significance of cor triatriatum dexter and dilated right atrium. Catheter Cardiovasc Interv 2000;51:186-91.
16. Harper RW, Mottram PM, McGaw DJ. Closure of secundum atrial septal defects with the Amplatzer septal occluder device: techniques and problems. Catheter Cardiovasc Interv 2002;57:508-24.
17. Kydd AC, McNab D, Calvert PA, Hoole SP, Rekhraj S, Sievert H, et al. The Eustachian ridge: not an innocent bystander. JACC Cardiovasc Imaging 2014;7:1062-3.
18. Silvestry FE, Kerber RE, Brook MM, Carroll JD, Eberman KM, Goldstein SA, et al. Echocardiography-guided interventions. J Am Soc Echocardiogr 2009;22:213-31. quiz 316-17.
19. Silvestry FE, Cohen MS, Armsby LB, Burkule NJ, Fleishman CE, Hijazi ZM, et al. Guidelines for the echocardiographic assessment of atrial septal defect and patent foramen ovale: from the American Society of Echocardiography and Society for Cardiac Angiography and Interventions. J Am Soc Echocardiogr 2015;28:910-58.
20. Bartel T, Muller S. Device closure of interatrial communications: peri-interventional echocardiographic assessment. Eur Heart J Cardiovasc Imaging 2013;14:618-24.
21. Lang RM, Badano LP, Tsang W, Adams DH, Agricola E, Buck T, et al. EAE/ASE recommendations for image acquisition and display using three-dimensional echocardiography. J Am Soc Echocardiogr 2012;25:3-46.
22. Hahn RT, Abraham T, Adams MS, Bruce CJ, Glas KE, Lang RM, et al. Guidelines for performing a comprehensive transesophageal echocardiographic examination: recommendations from the American Society of Echocardiography and the Society of Cardiovascular Anesthesiologists. J Am Soc Echocardiogr 2013;26:921-64.
23. Pushparajah K, Miller OI, Simpson JM. 3D echocardiography of the atrial septum: anatomical features and landmarks for the echocardiographer. JACC Cardiovasc Imaging 2010;3:981-4.
24. Simpson J, Lopez L, Acar P, Friedberg MK, Khoo NS, Ko HH, et al. Three-dimensional echocardiography in congenital heart disease: an expert consensus document from the European Association of Cardiovascular Imaging and the American Society of Echocardiography. J Am Soc Echocardiogr 2017;30:1-27.